JOURNAL OF Materials CHEMISTRY

The structures of the Ce and La N-phases $RE_3Si_{8-x}Al_xN_{11-x}O_{4+x}$ ($x \approx 1.75$ for RE = Ce, $x \approx 1.5$ for RE = La), determined by single-crystal X-ray and time-of-flight neutron powder diffraction, respectively

Jekabs Grins,* Zhijian Shen, Saeid Esmaeilzadeh and Pedro Berastegui

Department of Inorganic Chemistry, Arrhenius Laboratory, Stockholm University, SE–106 91 Stockholm, Sweden. Fax: +46 8 15 21 87; E-mail: mat@inorg.su.se

Received 13th March 2001, Accepted 23rd May 2001
First published as an Advance Article on the web 13th July 2001

Single crystals of the sialon Ce N-phase $Ce_3Si_{8-x}Al_xN_{11-x}O_{4+x}$ ($x \approx 1.75$) were obtained *via* a novel route, *i.e.* by first preparing a fully compacted body with phase constitutions far away from thermal dynamic equilibrium by means of a fast densification technique, spark plasma sintering, and then heat treating this compact in a sialon powder bed at 1600 °C in N_2 atmosphere for 24 h. The structure of the Ce N-phase was solved using MoKα single-crystal data and direct methods. It was refined in space group *I*2/*a* with $a = 15.798(1)$, $b = 4.8939(3)$, $c = 17.990(1)$ Å, $\beta = 114.816(4)°$, $V = 1262.4$ Å^3, to a weighted $R(F_{obs}^2) = 6.7\%$ for 977 unique reflections. The isostructural La phase structure was refined with anisotropic thermal parameters for La and N/O atoms using time-of flight neutron powder diffraction data. The structure exhibits three structural kinds of N/O anions: 4/15 of these are N atoms which are triangularly coordinated by 3 Si/Al atoms, 2/15 are tetrahedron free apex O atoms which are in addition bonded to 3 Ce/La atoms while the remaining 9/15 are on sites that are statistically occupied by N and O atoms and which are bonded to 2 tetrahedral Si/Al atoms and 1–2 Ce/La atoms. Comparisons are made with a previous structural proposal deduced from solid state nuclear magnetic resonance spectra.

Introduction

Sialons constitute a group of materials with both useful properties and unique structural features. Nitrogen-rich sialon phases have attracted great interest, especially β-sialon $Si_{6-z}Al_zO_zN_{8-z}$ and α-sialon $M_xSi_{12-(m+n)}Al_{(m+n)}O_nN_{16-n}$, in connection with the development of high-performance ceramic materials. Phase formation conditions and phase compatibility relationships have therefore been systematically studied in many M–Si–Al–O–N systems, *e g.* with M = Ca, Y, and rare-earth (RE) elements.[1] The structures of sialons represent also a significant extension to those of oxosilicates.[2] While oxosilicates only contain O atoms that are bound to none, one, or two Si atoms ($O^{[0]}$, $O^{[1]}$, $O^{[2]}$), N atoms are in nitridosilicates and sialons in addition found to be bound to three or four Si atoms ($N^{[3]}$, $N^{[4]}$).[3] Examples of unique structural features are edge-sharing SiN_4 tetrahedra in $BaSi_7N_{10}$,[4] $Ba_2Si_5N_6$[5] and octahedral coordination of Si by N in $Ce_{16}Si_{15}O_6N_{32}$.[6]

The existence of the so named N(ew) phase in the sialon systems RE–Si–Al–O–N with RE = Ce, La has been known for more than twenty years[7–9] but its structure has remained unsolved, largely due to the unavailability of single crystals. There have been controversies concerning its composition and unit cell. The composition for the Al free phases was initially believed to be $RE_2Si_6N_8O_3$ (or $RE_2O_3{\cdot}2Si_3N_4$)[7–9] while more recent studies have indicated it to be $RE_3Si_8N_{11}O_4$.[10,11] The X-ray powder diffraction (XRPD) pattern for the Ce N-phase has been indexed on basis of an *I*-centered monoclinic unit cell with $a = 16.288$, $b = 4.848$, $c = 7.853$ Å, $\beta = 91.54°$.[7] The cell is equivalent with a conventional *C*-centered cell with $a = 18.271$, $b = 4.848$, $c = 7.853$ and $\beta = 116.98°$.[12,13] The XRPD pattern for the La phase has also, from evidence of electron diffraction patterns, been indexed using a similar *C*-centered cell, however with a doubled *c*-axis: $a = 18.376$, $b = 4.873$, $c = 15.813$ Å and $\beta = 117.02°$[9] (JCPDS No. 36-570). The accordingly indexed pattern contains, however, only one single-indexed line, out of a total of 59 lines, with odd *l*. It can be noted here that the doubled cell can not, unlike the smaller cell, be transformed to a nearly orthogonal one and that transformation to an *I*-centered cell yields $a = 17.992$, $b = 4.873$, $c = 15.813$ Å and $\beta = 114.51°$.

The La N-phase has moreover been investigated in several studies by using magic-angle spinning nuclear magnetic resonance (NMR)[10,11,14–16] and a structure model has been proposed.[10,11,16] The model is not completely correct, as a comparison of the observed XRPD pattern and the pattern calculated from the model shows, but has very similar local atomic arrangements as the real structure.

The structure of the Ce N-phase $Ce_3Si_{6.25}Al_{1.75}N_{9.25}O_{5.75}$ has here been solved and refined using single-crystal (SC) X-ray data. The determination of the structure enabled a structure refinement of the analogous La phase $La_3Si_{6.5}Al_{1.5}N_{9.5}O_{5.5}$ using previously collected time-of-flight (TOF) neutron powder diffraction (NPD) data. A distribution of N and O atoms in the structure was determined from the neutron data which is in agreement with structural considerations and previous results from NMR.

Experimental

Single crystals of the Ce N-phase were obtained by heat treating a fully compacted body, prepared by spark plasma sintering (SPS), with phase constitutions far away from thermal dynamic equilibrium. Starting materials were Si_3N_4 (UBE, SN-E10), AlN (H.C. Starck, Berlin, grade A), Al_2O_3 (Alcoa, A16SG), dried La_2O_3 (≥99.9%, Johnson Matthey Chemicals Ltd.) and $Ce_2(CO_3)_3$ (Dr. Theodor Schuchardt, Gmbh & Co, Munchen). Corrections were made for the oxygen present in nitride precursors, *i.e.* the Si_3N_4 and AlN powders,

 DOI: 10.1039/b102340n

corresponding to 2.7 and 1.9 wt% of SiO_2 and Al_2O_3, respectively. Powder mixtures corresponding to compositions $RE_2Si_6N_8O_3$ and $RE_2Si_4Al_2N_6O_5$, with RE = Ce and La, were ball-mixed in water-free propanol for 24 h. The dried powder mixtures were loaded in a cylindrical carbon die with an inner diameter of 20 mm and compacted in vacuum in a spark-plasma sintering apparatus, Dr. Sinter 1050 (Sumitomo Coal Mining Co. Ltd., Japan), with the sintering process being monitored by a dilatometer. The samples were heated up from 600 °C, with a constant heating rate of 200 °C min^{-1} under a uniaxial pressure of 50 MPa, to a temperature at which full densification had taken place, which varied with composition between 1350 and 1450 °C, whereupon the SPS unit was turned off and the samples cooled at a rate of 400 °C min^{-1}.

The SPS compacted samples were characterized by XRPD with a Guinier–Hägg camera, using CuKα_1 radiation. The $RE_2Si_6N_8O_3$ samples were found to contain apatite phases $RE_{10}(SiO_4)_6N_2$ [9] and β-Si_3N_4, together with wollastonite related phases $RE_3Si_3O_6N_3$.[9] The Al containing $RE_2Si_4Al_2N_6O_5$ samples also contained $RE_{10}(SiO_4)_6N_2$ and β-Si_3N_4 together with perovskites $REAlO_3$. The microstructures of the samples were examined on polished surfaces in a JEOL JSM 880 scanning electron microscope (SEM) equipped with an energy-dispersive X-ray (EDX) micro-analysis system. The samples were found to contain no pores and consist of sub microcrystalline grains and an amorphous phase. They were subsequently heat-treated in a graphite furnace under a sialon powder bed at 1600 °C in N_2 atmosphere for 24 h. The obtained $Ce_2Si_4Al_2N_6O_5$ sample had, within the crust, a porous interior containing up to 100 μm large crystals. The corresponding La sample contained smaller but more well-shaped whisker-like crystals with uniform size, as shown in Fig. 1. The weight loss during the heat treatment for these samples was determined to be *ca.* 3%. XRPD patterns showed that the majority phase for the $RE_2Si_4Al_2N_6O_5$ compositions was of N type. The two Al-free samples were compact and contained only micron-size crystals. The $La_2Si_6N_8O_3$ sample contained, in addition to the N-phase, a large amount of an apatite phase plus β-sialon. The $Ce_2Si_6N_8O_3$ sample contained no N phase, but rather an apatite phase, a wollastonite phase, α- and β-sialon plus unidentified phase(s).

A powder mixture with a composition corresponding to $La_2Si_5AlN_7O_4$ was previously hot-pressed at 1800 °C for 2 h, yielding a sample with the La N-phase $La_3Si_{6.5}Al_{1.5}N_{9.5}O_{5.5}$ as the majority phase, and β-sialon.

Single-crystal XRD data for the Ce N-phase $Ce_3Si_{6.25}Al_{1.75}N_{9.25}O_{5.75}$ were collected with a STOE image-plate detector system, using a Siemens rotating anode and MoKα radiation. The distance between the crystal and the image plate was set to 70 mm, corresponding to a 2θ range up to 48° and *d*-values ≥ 0.88 Å. The STOE IPDS software package[17] was used for indexing and integration of the diffraction data, the X-RED[18]/X-SHAPE[19] programs for an absorption correction, SHELXS-86[20] for solving the structure by direct methods and SHELXL-97[21] for refining the structure against F^2.

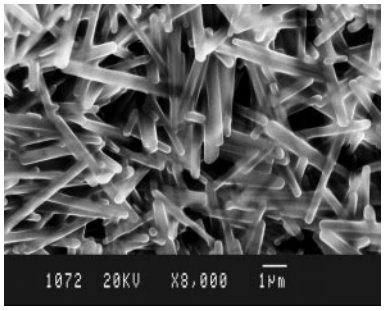

Fig. 1 Secondary-electron SEM micrograph of La N-phase crystallites in the sample with initial composition $La_2Si_6Al_2N_6O_5$.

CCDC reference number 166083. See http://www.rsc.org/suppdata/jm/b1/b102340n/ for crystallographic data in CIF or other electronic format.

TOF NPD data of $La_3Si_{6.67}Al_{1.33}N_{9.67}O_{5.33}$ were collected on the Polaris diffractometer at the UK spallation neutron source ISIS, Rutherford Appleton Laboratory. The Rietveld structure refinements were made with the GSAS program[22] and data from the high-resolution detector bank for *d* = 0.7–3.2 Å.

Results

Phase analysis and XRPD

The degree of substitution of Si by Al in the Ce N-phase was determined from 20 EDX point analyses on different crystals to be 22(1)%, *i.e.* somewhat less than that given by the nominal composition, giving a formula $Ce_3Si_{6.25}Al_{1.75}N_{9.25}O_{5.75}$. The XRPD reflections were sharp, with a half-width of 0.11° in 2θ at 50°. The pattern was indexed using an *I*-centered monoclinic unit cell with refined cell parameters $a = 15.798(1)$, $b = 4.8939(3)$, $c = 17.990(1)$ Å, $\beta = 114.816(4)°$, $V = 1262.4$ Å^3, using Si as internal standard, 72 reflections for $2\theta < 71°$ and, as needed, calculated intensities for the determined structure to assign indices. The indexed powder pattern is given in Table 1 for the first 20 observed lines. Systematic absences of reflections $h0l$, $h,l \neq 2n$ in the pattern agree with the space group *I*2/*a* (No. 15, *C*2/*c* conventionally). Only one of the first 20 reflections has *h* odd ($11\bar{2}$ with a relative intensity of 1%) and only 3 lines in the whole pattern were observed that could not be indexed with a cell with half the *a*-axis. This explains the controversies about the correct cell in the literature (refs. 2, 4, 8 and 9) and also, partly, why the structure has not been solved earlier from powder data. If the 3 weak lines with odd *h* are omitted, the pattern can not only be indexed with very high figures-of-merit with a smaller cell, but the *kl* indices then also imply a wrong lattice centering (*A* for the present cell). The determined unit cell parameters for the two La N phases in the samples with starting compositions $La_2Si_6N_8O_3$ and $La_2Si_6Al_2N_6O_5$ were respectively $a = 15.788(1)$, $b = 4.8688(5)$, $c = 17.977(2)$ Å, $\beta = 114.450(8)°$, $V = 1258.0$ Å^3 and $a = 15.863(1)$, $b = 4.9100(3)$, $c = 18.041(1)$ Å, $\beta = 114.903(7)°$, $V = 1274.5$ Å^3. The Al content in the latter phase was

Table 1 Observed and calculated 2θ values for the Guinier–Hägg diffraction pattern of $Ce_3Si_{6.25}Al_{1.75}N_{9.25}O_{5.75}$ up to the 20th observed line. $\Delta 2\theta = 2\theta_{obs.} - 2\theta_{calc.}$. $\lambda = 1.5406$ Å. Cell figure-of-merit: $M_{20} = 53$, $F_{20} = 96$ (0.0062, 34)

hkl	$2\theta_{obs}$/degrees	$\Delta 2\theta$	d_{obs}/Å	I/I_0
0 0 2	10.833	0.005	8.16	15
2 0 0	12.334	−0.002	7.17	10
0 1 1	18.912	−0.004	4.689	41
2 0 2	19.606	0.012	4.524	3
2 0 −4	19.995	0.003	4.437	24
1 1 −2	20.694	−0.015	4.289	1
2 1 −1	21.352	0.010	4.158	7
4 0 −2	22.503	0.003	3.948	27
2 1 −3	24.099	−0.001	3.690	24
4 0 0	24.822	0.004	3.584	7
2 0 4	29.369	0.021	3.039	67
4 1 −1	29.460	−0.004	3.030	93
4 1 −3	29.646	0.000	3.011	56
2 0 −6	29.796	−0.007	2.996	9
2 1 3	30.483	0.000	2.930	88
2 1 −5	30.836	0.000	2.897	100
4 0 2	31.150	−0.001	2.869	4
0 1 5	32.934	−0.013	2.717	16
4 1 1	33.219	0.005	2.695	14
4 1 −5	33.690	−0.013	2.658	19

determined from EDX analysis to be similar to that in the corresponding Ce phase and correspond to $x \approx 1.75$.

The XRPD pattern for the hot-pressed La N-phase sample showed it to contain also a β-sialon $Si_{6-z}Al_zO_zN_{8-z}$ phase. The unit cell parameters determined for the latter, $a = 7.6145(1)$ and $c = 2.9092(1)$ Å, correspond to a z-value of *ca.* 0.3(2), showing that the Al is preferentially incorporated in the N phase, which then has a derived composition $La_3Si_{6.5}Al_{1.5}N_{8.5}O_{5.5}$, corresponding to $x \approx 1.5$ in $La_3Si_{8-x}Al_xN_{11-x}O_{4+x}$. The determined unit-cell parameters were $a = 15.850(1)$, $b = 4.9029(4)$, $c = 18.039(1)$ Å, $\beta = 114.849(8)^\circ$, $V = 1272.0$ Å^3.

Refinement of the $Ce_3Si_{6.25}Al_{1.75}N_{9.25}O_{5.75}$ structure using SC XRD data

The Ce N-phase structure was solved using single-crystal data and direct methods. The conditions for intensity data collection and structure refinement are given in Table 2. The crystal used was of irregular form and with a size of 1.6×10^5 μm^3. Anisotropic thermal parameters were refined for Ce atoms. The Si and Al atoms were assumed to be randomly distributed over the available sites. Two anion sites were derived to be occupied by only N, one anion site by only O and the remaining anion sites to be statistically occupied by N and O atoms (see below). The refinement against F^2 converged at $R1 = 0.031$ for 62 refined parameters and 740 unique reflections with $F_{obs} > 4\sigma(F_{obs})$ and $wR2 = 0.067$ for all 977 unique reflections. The final thermal parameters and atomic coordinates are given in Table 3. The residual electron density was $+2.1$ e Å^{-3} (0.5 Å from Ce1) and -2.8 e Å^{-3} (1.0 Å from Ce1). The refined thermal parameter for Ce1, $U_{eq} = 0.0468(3)$ Å^2, is notably large in comparison with those for the other atoms and the thermal vibration ellipsoid is markedly elongated parallel with the c-axis. A refinement of the site occupancy factor for Ce1 did not however indicate any Ce vacancies and Fourier maps indicated no split positions. Selected bond distances are given in Table 4.

Table 2 Refinement data for $Ce_3Si_{6.25}Al_{1.75}N_{9.25}O_{5.75}$

Radiation (λ/Å)	Mo-Kα (0.71073)
μ/mm^{-1}	11.41
2θ/°	≤47.6
Data collected	h: −17–17; k: −5–5; l: −20–20
Total data	3715
Independent reflections	977
Observed independent reflections	740 [$F > 4\sigma(F)$]
R_{int}	0.027
Residuals[a] (all data)	$R_I = 0.045$ $wR_2 = 0.067$
Residuals [$F > 4\sigma(F)$]	$R_I = 0.031$ $wR_2 = 0.063$
GOF	1.045
$\Delta\rho_{max}$, $\Delta\rho_{min}$/e Å^{-3}	+2.1, −2.8 [Near Ce1]

[a] $R_I = \Sigma\|F_o| - |F_c\|/\Sigma|F_o|$; $wR_2 = [w(F_o^2 - F_c^2)/w(F_o^2)]^{1/2}$ with $w = 1/[\sigma^2(F_o^2) + (0.017P)^2 + 61.0P]$; $P = (\max(F_o^2, 0) + 2F_c^2)/3$.

Table 3 Atomic parameters for $Ce_3Si_{6.25}Al_{1.75}N_{9.25}O_{5.75}$; monoclinic, $a = 15.798(1)$, $b = 4.8939(3)$, $c = 17.990(1)$ Å, $\beta = 114.816(4)^\circ$, $V = 1262.4$ Å^3, $I2/a$, $Z = 4$; T = ($Si_{0.78}Al_{0.22}$) and X = ($N_{0.58}O_{0.42}$)

Atom	Site	x	y	z	U_{iso}, U_{eq}*/(Å$^2 \times 100$)
Ce1	4a	0	0	0	4.68(3)*
Ce2	8f	0.21100(3)	0.0046(1)	0.88356(3)	1.28(2)*
T1	8f	0.1435(2)	0.4792(6)	0.9789(1)	0.33(5)
T2	8f	0.3455(2)	0.5227(6)	0.8529(1)	0.39(5)
T3	8f	0.4954(2)	0.5538(5)	0.7997(1)	0.24(5)
T4	8f	0.3668(1)	0.0252(6)	0.7701(1)	0.37(5)
X1	8f	0.3954(5)	0.3931(15)	0.9501(4)	1.1(2)
X2	8f	0.4304(5)	0.1726(15)	0.6075(4)	1.0(2)
X3	8f	0.2307(4)	0.4527(15)	0.8205(4)	1.0(2)
X4	8f	0.6435(5)	0.3707(16)	0.6479(4)	1.4(2)
X5	4e	1/4	0.3372(21)	0	1.3(2)
N1	8f	0.3984(5)	0.3682(17)	0.7947(4)	0.9(2)
N2	8f	0.4447(5)	0.8461(16)	0.7409(5)	1.0(2)
O	8f	0.3536(4)	0.8146(13)	0.0232(4)	1.2(1)

Table 4 Bond distances (Å) for $Ce_3Si_{6.25}Al_{1.75}N_{9.25}O_{5.75}$

Ce1–	X1	2 × 2.448(7)	T1–	O	1.643(7)	T2–	X3	1.692(7)
	O	2 × 2.676(6)		X2	1.675(7)		X1	1.709(7)
	X4	2 × 2.749(7)		X1	1.686(7)		X4	1.713(9)
				X5	1.710(5)		N1	1.761(8)
Ce2–	O	2.481(6)	T3–	X2	1.691(7)	T4–	X3	1.713(7)
	X5	2.517(7)		N2	1.745(8)		X4	1.724(7)
	X3	2.547(7)		N1	1.750(8)		N1	1.754(9)
	X4	2.670(7)		N2	1.760(8)		N2	1.761(8)
	O	2.738(6)						
	X2	2.795(7)	X1–	T1	1.686(7)	X2–	T1	1.675(7)
	X3	2.995(7)		T2	1.709(7)		T3	1.691(7)
				Ce1	2.448(7)		Ce2	2.795(7)
X3–	T2	1.692(7)	X4–	T2	1.713(9)	X5–	T1	2 × 1.710(5)
	T4	1.713(7)		T4	1.724(7)		Ce2	2 × 2.517(7)
	Ce2	2.547(7)		Ce2	2.670(7)			
	Ce2	2.995(7)		Ce1	2.749(7)			
N1–	T3	1.750(8)	N2–	T3	1.745(8)	O–	T1	1.643(7)
	T4	1.754(8)		T3	1.760(8)		Ce2	2.481(6)
	T2	1.761(8)		T4	1.761(8)		Ce1	2.676(6)
							Ce2	2.738(6)

Refinement of the $La_3Si_{6.5}Al_{1.5}N_{9.5}O_{5.5}$ structure using TOF NPD data

A Rietveld structure refinement of $La_3Si_{6.5}Al_{1.5}N_{9.5}O_{5.5}$, with 37 positional parameters, 14 isotropic thermal displacement parameters, 1887 reflections for $d = 0.7$–3.2 Å, and a total of 78 refined parameters, converged with $\chi^2 = 1.8$ and $R_F = 1.0\%$. The β-sialon phase in the sample was included in the refinement with atomic coordinates from Grün,[23] with a refined weight fraction of 10.1%. Allowance for 52 anisotropic thermal displacement parameters for Ce and O/N atoms in a corresponding refinement with 130 refined parameters yielded an improved fit between the observed and calculated patterns, with $\chi^2 = 1.04$ and R-values of $R_{wp} = 1.2\%$, $R_p = 2.6\%$, $DwD = 0.64$ and $R_F = 0.5\%$. The fit between observed and calculated intensities is illustrated in Fig. 2. The obtained atomic positions and thermal parameters are given in Table 5 and bond distances in Table 6.

Structure description and the distribution of O and N atoms

The refined atomic parameters and bond distances are very similar for the Ce and La phases and the structure is therefore here described only for the Ce compound. The N-phase

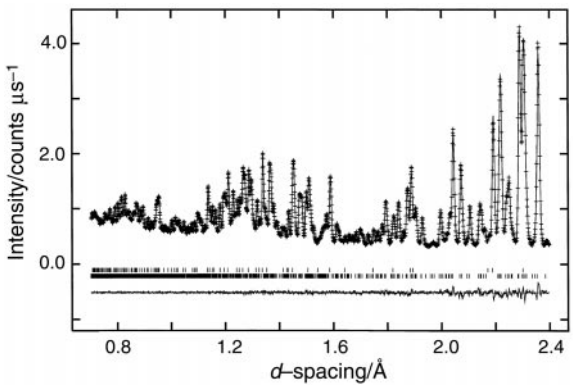

Fig. 2 Observed (crosses), calculated (solid line) and difference (bottom) TOF NPD pattern of the La N-phase $La_3Si_{6.5}Al_{1.5}N_{9.5}O_{5.5}$ for $d = 0.7$–2.4 Å. The upper set of reflection markers are for the β-sialon impurity phase.

Table 5 Atomic parameters for $La_3Si_{6.5}Al_{1.5}N_{9.5}O_{5.5}$; monoclinic, $a=15.850(1)$, $b=4.9029(4)$, $c=18.039(1)$ Å, $\beta=114.849(8)^\circ$, $V=1272.0$ Å^3, $I2/a$, $Z=4$; T = $(Si_{0.81}Al_{0.19})$ and X = $(N_{0.56}O_{0.44})$

Atom	Site	x	y	z	U_{iso}, U_{eq}*/(Å$^2\times100$)
La1	4a	0	0	0	5.37*
La2	8f	0.2111(1)	0.0037(4)	0.8828(1)	1.57*
T1	8f	0.1433(3)	0.4821(7)	0.9791(2)	0.65(7)
T2	8f	0.3449(3)	0.5255(7)	0.8530(2)	0.65(6)
T3	8f	0.4961(2)	0.5543(6)	0.8009(2)	0.53(8)
T4	8f	0.3667(2)	0.0203(7)	0.7696(2)	0.57(6)
X1	8f	0.3945(2)	0.3980(4)	0.9494(2)	2.26*
X2	8f	0.4309(2)	0.1708(5)	0.6067(1)	2.14*
X3	8f	0.2299(1)	0.4621(4)	0.8194(1)	1.65*
X4	8f	0.6417(1)	0.3729(4)	0.6476(1)	0.82*
X5	4e	1/4	0.3444(6)	0	0.52*
N1	8f	0.3982(1)	0.3665(4)	0.7951(1)	1.38*
N2	8f	0.4461(1)	0.8473(3)	0.7415(1)	1.36*
O	8f	0.3533(2)	0.8163(6)	0.0220(2)	1.30*

Table 6 Bond distances (Å) for $La_3Si_{6.5}Al_{1.5}N_{9.5}O_{5.5}$

La1–	X1	2 × 2.471(2)	T1–	O	1.633(4)	T2–	X3	1.684(4)
	O	2 × 2.665(3)		X2	1.671(4)		X1	1.693(4)
	X4	2 × 2.728(2)		X1	1.681(4)		X4	1.710(4)
				X5	1.703(4)		N1	1.770(4)
La2–	O	2.504(3)	T3–	X2	1.674(4)	T4–	X3	1.686(4)
	X5	2.550(3)		N2	1.739(4)		X4	1.709(3)
	X3	2.586(3)		N1	1.762(4)		N1	1.768(4)
	X4	2.678(3)		N2	1.761(4)		N2	1.754(4)
	O	2.724(5)						
	X2	2.820(3)	X1–	T1	1.681(4)	X2–	T1	1.671(4)
	X3	2.944(3)		T2	1.693(4)		T3	1.674(4)
				La1	2.471(2)		La2	2.820(3)
X3–	T2	1.684(4)	X4–	T2	1.710(4)	X5–	T1	2 × 1.703(4)
	T4	1.686(4)		T4	1.709(3)		La2	2 × 2.550(3)
	La2	2.586(3)		La2	2.678(3)			
	La2	2.944(3)		La1	2.728(2)			
N1–	T3	1.762(4)	N2–	T3	1.739(4)	O–	T1	1.633(4)
	T4	1.768(4)		T3	1.761(4)		La2	2.504(3)
	T2	1.770(4)		T4	1.754(4)		La1	2.665(3)
							La2	2.724(4)

structure is illustrated in Fig. 3 in a projection on the *ac*-plane. It contains, as structural units, ribbons with composition T_6X_{14} that extend along the *b*-axis and are formed by corner-sharing TX_4 tetrahedra (T = T2, T3, T4). A separate ribbon is illustrated in Fig. 4. The anions in the central part of the ribbon are N1 and N2 atoms that connect three T tetrahedra,

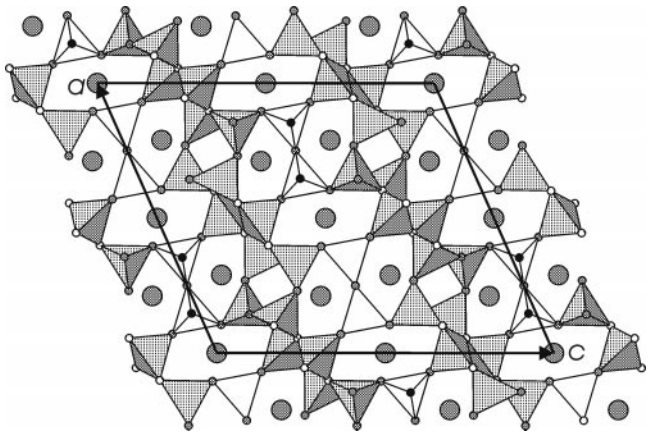

Fig. 3 Illustration of the tetrahedral framework of the Ce N-phase structure projected on the (101) plane. The positions of the Ce atoms are shown by the larger hatched circles and the positions of the N, O and mixed O/N anion sites by smaller open, filled and hatched circles, respectively. The tetrahedra belonging to T_6X_{14} ribbons are hatched.

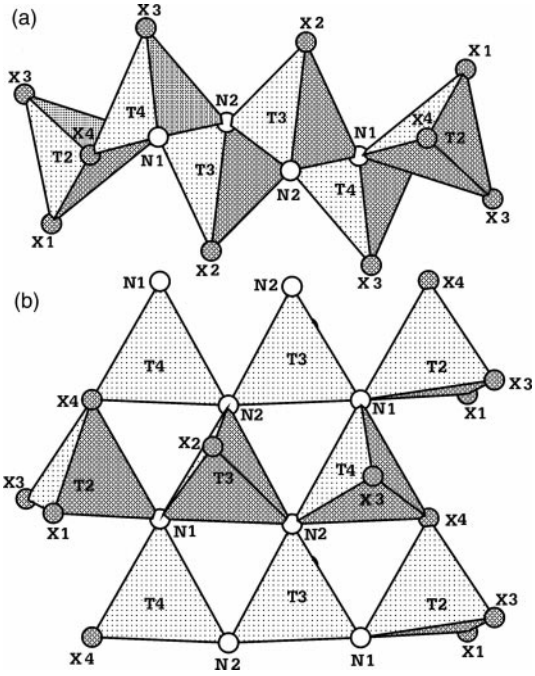

Fig. 4 Illustration of T_6X_{14} ribbons in the N-phase structure: (a) projected on the (101) plane and (b) the (001) plane. The N atom and mixed O/N atom sites are illustrated by open and hatched circles, respectively.

while the outer anion sites are X1–X4 with a mixed occupancy of N and O atoms. Each ribbon corner-shares 4 of the outer anions with 2 other ribbons, thus forming (100) layers of tetrahedra, and the other 4 with 2 T_2X_7 (T = T1) units. The two tetrahedra in the T_2X_7 unit are connected by the X5 atom and each has one free apex O atom. There are thus 3 structural types of anions: (i) the N atoms in the inner part of the T_6X_{14} ribbons that are (mainly, see below) bonded to 3 T atoms; (ii) the N/O atoms that are bonded to two T atoms plus 1–2 Ce atoms (X1, X2 to 1 Ce atom and X3, X4, X5 to 2 Ce atoms); and (iii) the free apex O atom of the T1 tetrahedra that is bonded to 3 Ce atoms. The latter coordination is not uncommon for sialons and is found for the åkermanite type phases $RE_2O_3{\cdot}Si_3N_4$[24] and in the U-phase $RE_3Al_{3+x}Si_{3-x}O_{12+x}N_{2-x}$ structure.[25] The coordinations of the Ce atoms are illustrated in Fig. 5. The Ce1 atom is octahedrally coordinated at distances of 2.45–2.75 Å by 4 equatorial X atoms and 2 O atoms. The large thermal displacement of Ce1 is predominantly in the *c*-axis direction. The Ce2 atom is surrounded at distances of 2.48–3.04 Å by 8 anions (5X + 2O + 1N) that approximately form a cubic antiprism. Two bond distances are however for this description of the coordination polyhedron long (3.00 Å to X3 and 3.04 Å to N1) in comparison with the others, $\leqslant$2.79 Å, and imply that the N1 atom is bonded not only to 3 T atoms but also weakly to the Ce2 atom.

The above described distribution of N and O atoms on the

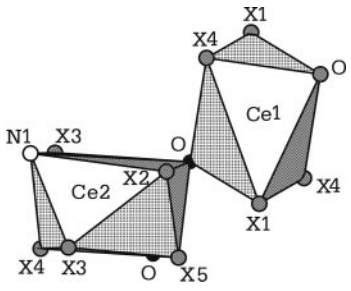

Fig. 5 Coordination polyhedra for the Ce atoms in the Ce N-phase structure. The positions of the N, O and mixed O/N anion sites are shown by smaller open, filled and hatched circles, respectively.

available anion sites was, in the case of the La phase, directly determinable due to the distinctly different neutron scattering amplitudes of N (0.94×10^{-12} cm) and O (0.58×10^{-12} cm). Alternative distributions yielded poorer agreements with the observed pattern and implausible thermal parameters for sites N1, N2 and O. Smaller variations of the N/O ratio for the mixed X sites can however not be ruled out.

The derived distribution of N and O atoms is also in agreement with expected bond distances, distributions in other sialon structures and NMR data (see below). The observed distances fall into three groups; the T1–O distance 1.64 Å, T–X distances between 1.68–1.73 Å (mean 1.70 Å), and T–N distances of 1.76 Å. Expected distances may be calculated using effective ionic radii in nitrides (coordination number in parentheses)[26] of N^{3-}(III) = 1.44 Å, N^{3-}(II) = 1.42 Å, Si^{4+}(IV) = 0.29 Å, Al^{3+}(IV) = 0.41 Å, effective ionic radii for oxygen ions[27] of O^{2-}(III) = 1.36 Å, O^{2-}(II) = 1.35 Å; yielding 1.64 Å for T1–O, 1.71 Å for T–X and 1.76 Å for T–N.

Discussion

The N-phase structure illustrates well the difference in tetrahedral frameworks between those found for nitridosilicates or sialons and the more common oxosilicates. For structures of the former the frameworks are frequently more connected, and thus more rigid, as a consequence of that N atoms connect three or four Si tetrahedra.

The long time for which the N-phase structure has remained unsolved can here, in retrospect, be attributed to the unavailability of single crystals and the difficulty to discern the framework superstructure along the *c*-axis by XRPD, *i.e.* to select the correct unit cell.

The N-phase has been subjected to investigation by NMR in a series of papers.[10,11,14–16] From the NMR data, and using the correct composition $RE_3Si_8N_{11}O_4$, it has been deduced that per formula unit there are: (i) 4 N on N–Si_3 sites, (ii) 2 O on O–Si sites that are bonded in addition to 3 RE atoms, (iii) 9 (N/O) atoms on (N/O)–Si_2 sites. These findings are in complete agreement with the structure as solved here from SC XRD data and show how powerful a tool solid state NMR can be to resolve structural issues. In the present case the NMR data also confirm the determined distribution of O and N from NPD. A complete structure model for the N-phase has been proposed[10,11,16] on basis of the NMR data, however using an incorrect unit cell with half the volume of the true one. The proposed model does not agree well with our observed neutron and X-ray powder patterns. A comparison with the solved structure shows that this model contains many structure features that are present in the structure as determined from single-crystal data, but there are also several differences in how structure elements are interconnected, reflecting the considerable difficulty to elucidate a correct structure from a knowledge of only some local configurations.

The method used in this study to prepare single crystals of the Ce N-phase, a post heat treatment of SPS sintered samples, is novel and offers good prospects to obtain single crystals, as well as good crystallized samples for powder work, of other sialon phases. There are several beneficial factors involved, including: (i) the SPS compacted samples have maximum density which minimizes losses by evaporation and provides for reactivity by a good contact between phases, (ii) small crystalline grains are distributed evenly throughout a glass phase, facilitating a dissolution of N into the glass and thus a growth of phases in it, (iii) the glass phase is retained around the immersed crystallites by adhesion, providing for a homogeneous sample in the early stages of reactions. The vast majority of single crystals of nitridosilicates and sialons have so far been obtained using alkaline earth or rare earth metal melts.[2] The crystals grown by our method are of excellent quality, although the growth mechanism appears not to be fully known. The process applied in the present work may, however, be an alternative and competitive route to prepare nitridosilicate compounds, and we are presently exploring this possibility.

Acknowledgements

The authors thank Prof. M. Nygren for support and valuable discussions. This work has been financially supported by the Swedish Natural Science Foundation.

References

1 T. Ekström and M. Nygren, *J. Am. Ceram. Soc.*, 1992, **75**, 259.
2 W. Schnick and H. Huppertz, *Chem. Eur. J.*, 1997, **3**, 679.
3 F. Liebau, *Angew. Chem., Int. Ed.*, 1999, **38**, 1733.
4 H. Huppertz and W. Schnick, *Chem. Eur. J.*, 1997, **3**, 249.
5 H. Yamane and F. J. DiSalvo, *J. Alloys Compd.*, 1996, **240**, 33.
6 K. Köllisch and W. Schnick, *Angew. Chem., Int. Ed.*, 1999, **38**, 357.
7 T.-I. Mah, K. S. Mazdiyasni and R. Ruh, *J. Am. Ceram. Soc.*, 1979, **62**, 12.
8 R. R. Wills, R. W. Stewart, J. A. Cunningham and J. M. Wimmer, *J. Mater. Sci.*, 1976, **11**, 749.
9 M. Mitomo, F. Izumi, S. Horiuchi and Y. Matsui, *J. Mater. Sci.*, 1982, **17**, 2359.
10 D. P. Thompson, M. J. Leach and R. K. Harris, *C-MRS Int. Symp. Proc. 2*, 1990, p. 435.
11 R. K. Harris, M. J. Leach and D. P. Thompson, *Chem. Mater.*, 1992, **4**, 260.
12 P. E. D. Morgan, *J. Am. Ceram. Soc.*, 1979, **62**, 636.
13 J. W. Visser, G. G. Johnson Jr. and R. Ruh, *J. Am. Ceram. Soc.*, 1979, **62**, 636.
14 R. K. Harris, M. J. Leach and D. P. Thompson, *Chem. Mater.*, 1989, **1**, 336.
15 R. Dupree, M. H. Lewis and M. E. Smith, *J. Am. Chem. Soc.*, 1989, **111**, 5125.
16 R. K. Harris and P. R. Bodart, *Mater. Sci. Forum*, 2000, **325–326**, 305.
17 STOE IPDS software manual, version 2.87, Darmstadt, Germany, December 1997.
18 STOE & Cie GmbH, Darmstadt, Germany, 1996, v. 1.07.
19 STOE & Cie GmbH, Darmstadt, Germany, 1996, v. 1.01.
20 G. M. Sheldrick, *SHELXS-86, Program for crystal structure determination*, University of Göttingen, Germany, 1986.
21 G. M. Sheldrick, *SHELXL-97, Program for crystal structure determination*, University of Göttingen, Germany, 1997.
22 A. C. Larson and R. B. Von Dreele, Los Alamos National Laboratory Report No. LA-UR-86-748, Los Alamos, NM, 1987.
23 R. Grün, *Acta Crystallogr., Sect. B*, 1979, **35**, 800.
24 P. Appendino and M. Montorsi, *J. Less-Common Met.*, 1979, **64**, 303.
25 P.-O. Käll, J. Grins and M. Nygren, *Acta Crystallogr., Sect. C*, 1991, **47**, 2015.
26 W. H. Bauer, *Cryst. Rev.*, 1987, **1**, 59.
27 R. D. Shannon, *Acta Crystallogr., Sect. A*, 1976, **32**, 751.